

# Influence of elasticity parameters and direction of material axes on velocity of R-waves in thin composite panel

T. Kroupa<sup>a,\*</sup>, J. Červ<sup>b</sup>

<sup>a</sup>*Institute of Thermomechanics, Czech Academy of Sciences, Veveřská 11, 301 14 Plzeň, Czech Republic*

<sup>b</sup>*Institute of Thermomechanics, Czech Academy of Sciences, Dolejškova 5, 182 00 Praha 8, Czech Republic*

Received 29 August 2008; received in revised form 5 September 2008

---

## Abstract

The paper is aimed at the determination of Rayleigh wave velocity at the edge of a thin unidirectional carbon-epoxy composite panel. Velocities are calculated for various fiber angles and elasticity parameters. Numerical simulation is performed using finite element analysis. Results from the numerical analysis are compared with experimental results and analytical solution.

© 2008 University of West Bohemia in Pilsen. All rights reserved.

*Keywords:* Composites, Rayleigh-edge waves, FEA

---

## 1. Introduction

The problem concerned with Rayleigh-edge wave propagation in a long-fiber reinforced composite is discussed in the paper. The considered composite material is epoxy resin (matrix) reinforced by long carbon fibers, which are systematically arranged in the matrix in specified direction. Since the fibers are systematically oriented, a composite of this kind has strong directional dependency of material properties, thus macroscopically for sufficiently long wavelength, it can be regarded as a homogeneous orthotropic material.

The propagation of elastic waves in anisotropic media differs in many aspects from that customarily attributed to elastic waves in isotropic media. This fact is evident from results presented in e.g. [4, 7, 10] or [11]. For a given direction of wave propagation represented by a wave vector there will be generally three phase velocities [1], the three corresponding displacement (polarization) vectors will be mutually orthogonal, but contrary to the isotropic case the displacements are neither truly longitudinal nor truly transverse in character. As the mechanical or material behavior of the solid becomes more complicated, the description of non-stationary wave propagation starts to be analytically intractable and, consequently, such problems are often modeled by means of discretization techniques such as finite elements (FE) or finite differences. It is very useful to supplement the theoretical analysis by experimentally obtained results.

The paper is aimed at the Rayleigh wave propagation along an edge of a thin orthotropic laminate panel loaded in-plane by stress pulse. Rayleigh waves or R-waves propagate along the loaded edge of the material. Under above conditions R-waves bear significant amount of the energy, taken relatively to the amount of the energy propagated by other types of the waves (quasi-longitudinal and quasi-transverse). It is the most significant characteristic of the R-waves

---

\*Corresponding author. Tel.: +420 377 632 367, e-mail: kroupa@kme.zcu.cz.

that they are located closely to the free edge of the material and vanish with the increasing distance from the loaded edge. The propagation velocity of the R-waves along the loaded edge depends on the fiber angle. This can be easily anticipated with respect to the direction dependence of the material properties of the composite. Some basic research in the field of R-wave propagation in thin orthotropic composite panel was performed in [2, 3, 4].

Experimental solution of the given problem utilizes for non-contact measurements a laser vibrometer. Theoretical solution is based on finite element analysis and analytical approach. The comparison of the numerical, experimental and analytical (theoretical) results is presented and discussed in the paper.

## 2. Problem formulation

Let us consider a thin unidirectional fiber-reinforced composite panel. It is also assumed that fiber diameter and thickness of the composite panel are small compared to the shortest wavelength taken into account. Hence one can consider the material as orthotropic in the state of plane stress. The principal directions of orthotropy often do not coincide with coordinate directions that are geometrically natural to the solution of the problem. Therefore it is assumed that body axes  $x, y$  form a nonzero angle  $\vartheta$  with principal material axes  $L$  (longitudinal),  $T$  (transverse) as may be seen in fig. 1. Third axis  $z$  is identical with material axis  $T'$  and constitutes axis of rotation of principal material axes  $L, T$  from body axes  $x, y$  (fig. 1).

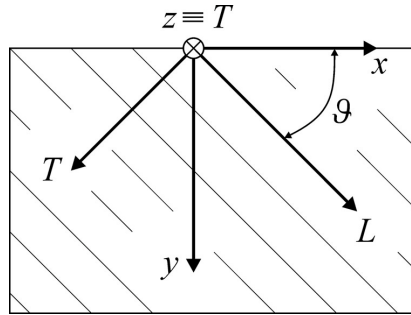


Fig. 1. Unidirectional composite panel

The stress-strain relation for plane stress in principal material axes  $L, T$  can be written in the form [6]

$$\begin{pmatrix} \sigma_L \\ \sigma_T \\ \tau_{LT} \end{pmatrix} = \begin{bmatrix} C_{11} & C_{12} & 0 \\ C_{12} & C_{22} & 0 \\ 0 & 0 & C_{66} \end{bmatrix} \cdot \begin{pmatrix} \varepsilon_L \\ \varepsilon_T \\ \gamma_{LT} \end{pmatrix}, \quad (1)$$

where matrix elements  $C_{ij}$  depend on Young's moduli and Poisson's ratios (for explicit expressions see e.g. [6]),  $\sigma_L, \sigma_T$  and  $\tau_{LT}$  are normal stresses and shear stress in material axes coordinate system and  $\varepsilon_L, \varepsilon_T$  and  $\gamma_{LT}$  strains and shear strain also in material axes coordinate system. Stress-strain relation in  $x, y$  coordinate system can be written in the form

$$\begin{pmatrix} \sigma_x \\ \sigma_y \\ \tau_{xy} \end{pmatrix} = \begin{bmatrix} Q_{11} & Q_{12} & Q_{16} \\ Q_{12} & Q_{22} & Q_{26} \\ Q_{16} & Q_{26} & Q_{66} \end{bmatrix} \cdot \begin{pmatrix} \varepsilon_x \\ \varepsilon_y \\ \gamma_{xy} \end{pmatrix}, \quad (2)$$

where matrix elements  $Q_{ij}$  depend on elements  $C_{ij}$  and fiber direction angle  $\vartheta$  (for further details see e.g. [6]). The displacements equations of motion in the absence of body forces are [4]

$$Q_{11} \frac{\partial^2 u}{\partial x^2} + 2Q_{16} \frac{\partial^2 u}{\partial x \partial y} + Q_{66} \frac{\partial^2 u}{\partial y^2} + Q_{16} \frac{\partial^2 v}{\partial x^2} + (Q_{12} + Q_{66}) \frac{\partial^2 v}{\partial x \partial y} + Q_{26} \frac{\partial^2 v}{\partial y^2} = \rho \frac{\partial^2 u}{\partial t^2}, \quad (3)$$

$$Q_{66} \frac{\partial^2 v}{\partial x^2} + 2Q_{26} \frac{\partial^2 v}{\partial x \partial y} + Q_{22} \frac{\partial^2 v}{\partial y^2} + Q_{16} \frac{\partial^2 u}{\partial x^2} + (Q_{12} + Q_{66}) \frac{\partial^2 u}{\partial x \partial y} + Q_{26} \frac{\partial^2 u}{\partial y^2} = \rho \frac{\partial^2 v}{\partial t^2}, \quad (4)$$

where  $t$  stands for time,  $u$  and  $v$  are displacements in the axes  $x$  and  $y$  respectively,  $\rho$  is material density. The in-plane loading is applied to the upper edge (see fig. 3). The time and space distribution of the loading may be given by arbitrary function. The lower and both lateral edges are traction-free. At the beginning the strip is at rest (zero initial conditions) and without any stress. Displacement  $u$  and  $v$  constitute displacement vector ( $\mathbf{u} = [u, v]^T$ ).

In the case of plane stress and for a given direction of wave propagation there will be two phase velocities. Values of the phase velocities of quasi-longitudinal ( $c_L$ ) and quasi-transverse ( $c_T$ ) waves, which propagate in the direction of material axis  $L$  and quasi-longitudinal wave ( $c_{L'}$ ) in the direction of material axis  $T$  are shown in the tab. 1. They are obtained from the relations

$$c_L = \sqrt{\frac{E_L}{\rho(1 - \nu_{LT}^2 \frac{E_T}{E_L})}}, \quad (5)$$

$$c_{L'} = \sqrt{\frac{E_T}{\rho(1 - \nu_{LT}^2 \frac{E_T}{E_L})}}, \quad (6)$$

$$c_T = \sqrt{\frac{G_{LT}}{\rho}}, \quad (7)$$

where  $E_L$  is Young’s modulus in the fiber direction,  $E_T$  is Young’s modulus in the transverse direction to the fibers,  $G_{LT}$  is shear modulus in the plane of the composite panel and  $\nu_{LT}$  is Poisson’s ratio. R-waves propagate closely to the free edge of the material and vanish with the increasing distance from the loaded edge.

Two sets of the elasticity constants were used for the FE analysis (see tab. 1). The first set was obtained from the precise analysis of the experimental results, taken from the experiment, which was performed with the use of the laser pulse loading. The second set was given by the manufacturer.

Table 1. Wave velocities for both sets of the material constants

Constant [units]	1 <sup>st</sup> set	2 <sup>nd</sup> set	Velocity [units]	1 <sup>st</sup> set	2 <sup>nd</sup> set
$E_L$ [GPa]	114.20	113.80	$c_L$ [ $\text{ms}^{-1}$ ]	8 637.50	8 622.50
$E_T$ [GPa]	8.80	8.80	$c_{L'}$ [ $\text{ms}^{-1}$ ]	2 397.70	2 397.70
$G_{LT}$ [GPa]	5.15	4.80	$c_T$ [ $\text{ms}^{-1}$ ]	1 828.70	1 765.50
$\nu_{LT}$ [-]	0.28	0.28	$c_R^{(0^\circ)}$ [ $\text{ms}^{-1}$ ]	1 804.60	1 745.10
$\rho$ [ $\text{kgm}^{-3}$ ]	1 540.00	1 540.00	$c_R^{(90^\circ)}$ [ $\text{ms}^{-1}$ ]	1 779.20	1 726.30

The velocities of the Rayleigh waves for fiber directions  $0^\circ$  and  $90^\circ$  are also shown in the tab. 1. The determination of  $c_R$  for chosen materials is closely discussed in [2] or [3]. Let us remind, that velocity  $c_R$  considerably depends on the fiber direction in the case of composite material.

### 3. Experiment

The experimentally investigated values of fiber angle dependence of R-wave velocity were obtained with the use of Compact Laser Vibrometer 2000 (CLV) with two measuring sensor heads. The edge of the composite panel was loaded by laser light pulse. Time dependence of transverse velocity  $\frac{\partial v}{\partial t}$  at loaded edge was measured in two chosen distances from the loading point. Each time dependence that corresponds to R-wave pulse has one minimum. R-wave velocity was calculated as ratio of sensor heads distance and time difference between minima of corresponding R-wave pulses. Experiments were performed on in-plane loaded square composite panels with dimensions  $501 \text{ mm} \times 501 \text{ mm} \times 2.2 \text{ mm}$  (see [4]).

### 4. Finite element analysis

For generation of R-wave pulse in FE analysis the time dependence of the loading force was chosen in the shape depicted in fig. 2.

The dimensions of numerically investigated model are not the same as the dimensions of experimentally investigated panel. Due to avoiding of the wave reflections the exact dimensions of panel modeled by FEA are  $1500 \text{ mm} \times 1000 \text{ mm} \times 2 \text{ mm}$  (see fig. 3).

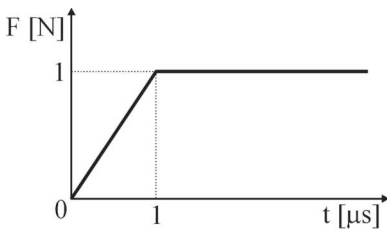


Fig. 2. Time dependence of the loading force

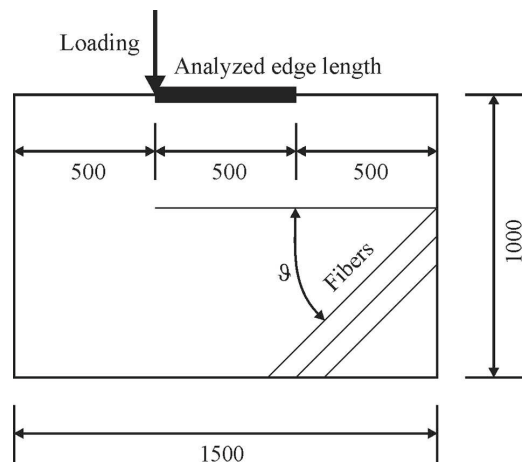


Fig. 3. Dimensions of FE model [mm]

The software at our disposal has limitation for the number of elements (cca 500 000). With respect to the model dimensions the FE mesh of the panel can not be equidistant. The mesh is therefore biased. Elements have the dimensions  $1 \text{ mm} \times 1 \text{ mm}$  near the loaded edge (5 layers). The edge length of the elements parallel to the loaded edge is 1 mm along the whole edge (i.e. 1500 mm) of the panel. The edge length in the direction perpendicular to the loaded edge of the panel is increasing with increasing distance from the loaded edge. The number of

the elements in the model is 450 000. The spatial discretization was performed using bilinear square elements.

The Single Step Houbolt scheme [5] for time integration (with default values given in [5]) is used in the work. Vectors of displacement, velocity and acceleration can be calculated from the set of equations

$$\left(\frac{2}{\Delta t^2}\mathbf{M} + \mathbf{K}\right) \Delta \mathbf{u} = \mathbf{F}^{n+1} + \mathbf{M}\mathbf{a}^n - \mathbf{K}\mathbf{u}^n + \frac{2}{\Delta t^2}\mathbf{M}\left(\Delta t\mathbf{v}^n - \frac{1}{2}\Delta t^2\mathbf{a}^n\right), \quad (8)$$

$$\mathbf{u}^{n+1} = \mathbf{u}^n + \Delta \mathbf{u}, \quad (9)$$

$$\mathbf{u}^{n+1} = \mathbf{u}^n + \Delta t\mathbf{v}^n - \frac{1}{2}\Delta t^2\mathbf{a}^n + \Delta t^2\mathbf{a}^{n+1}, \quad (10)$$

$$\mathbf{v}^{n+1} = \mathbf{v}^n - \frac{1}{2}\Delta t\mathbf{a}^n + \frac{3}{2}\Delta t\mathbf{a}^{n+1}, \quad (11)$$

where  $\mathbf{M}$  is mass matrix (full mass matrix is used in the analyzes in the paper),  $\mathbf{K}$  is stiffness matrix,  $\mathbf{F}$  is vector of loading forces,  $n$  is index denoting the number of time increment,  $\Delta t$  time increment,  $\mathbf{u}$  is vector of nodal displacements,  $\mathbf{v}$  is vector of nodal velocities,  $\mathbf{a}$  is vector of nodal accelerations and  $\Delta \mathbf{u}$  is vector of nodal displacements increments. Integration time step  $\Delta t$  is taken as  $0.1 \mu\text{s}$ . The whole number of the integration time steps is 2 000, which gives total analysis time  $T = 200 \mu\text{s}$ .

The R-wave velocities are calculated for fiber angles from  $0^\circ$  to  $180^\circ$  with step  $5^\circ$ . The length, where the calculation of R-wave velocities is performed, is the middle third of the panel (see fig. 3).

The determination of the R-wave velocity begins with analysis of transverse velocities pathplots along the analyzed loaded edge for all time increments. The typical transverse velocity pathplots are shown in the fig. 4 and fig. 5. The minimum, which represents R-wave peak, is pointed out.

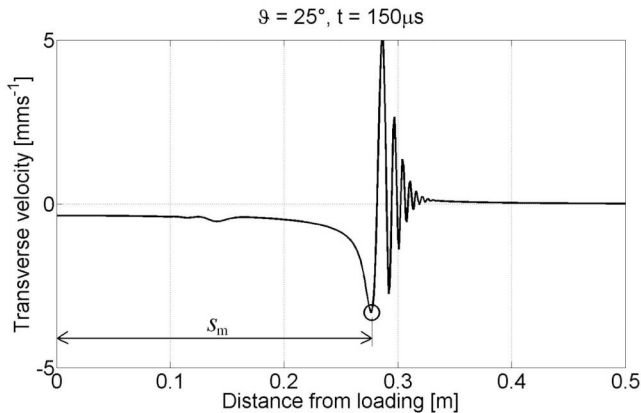


Fig. 4. Transverse velocity pathplot along the loaded edge for given time and fiber angle ( $\circ$  – minimum,  $t = 150 \mu\text{s}$ ,  $\vartheta = 25^\circ$ , 1<sup>st</sup> set of material constants)

Once the minima are found for all time increments, the distance from the loading point  $s_m$  and the time  $t_m$  can be put into one graph. The time in this case means

$$t_m = t_i - t_0, \quad (12)$$

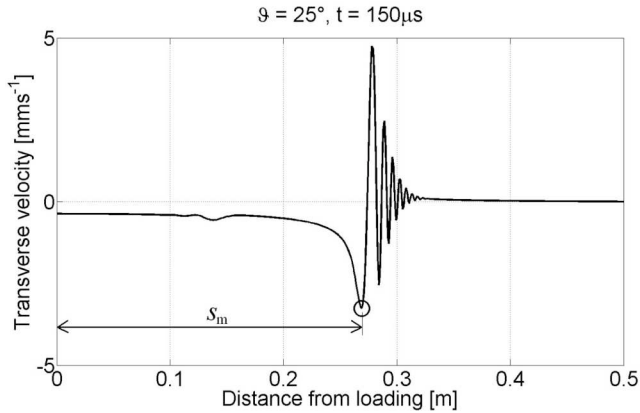


Fig. 5. Transverse velocity pathplot along the loaded edge for given time and fiber angle ( $\circ$  – minimum,  $t = 150 \mu\text{s}$ ,  $\vartheta = 25^\circ$ , 2<sup>nd</sup> set of material constants)

where  $t_i$  is the time of analyzed time increment and  $t_0$  is the time of the moment when the transverse velocity pathplot has the suitable shape for determination of the minimum (see fig. 6 and fig. 7). The line can be interpolated through this data. The slope of the line is the sought-after velocity of the R-wave for given fiber direction. An examples of the graph mentioned above for the fiber direction  $25^\circ$  are shown in the fig. 6 and fig. 7. It was found out that for all considered fibre angles and sets of material constants the interpolating curve is always straight line such as in fig. 6 and fig. 7. It means that looked for velocity is constant for the given fibre angle and therefore the problem is said to be non-dispersive.

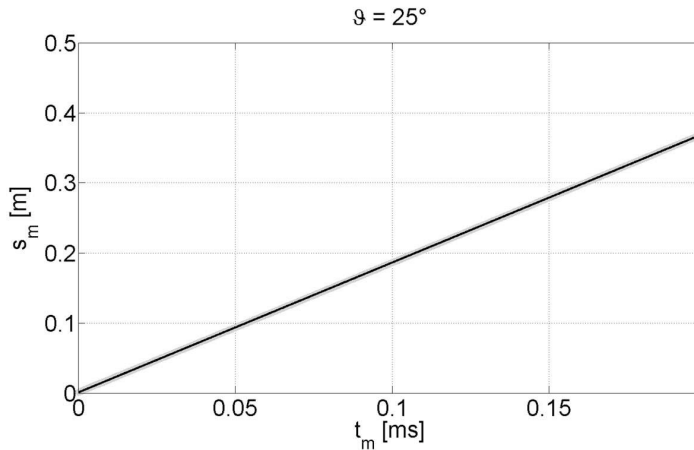


Fig. 6. Distance of R-wave pulse minimum from the loading point vs. time ( $\vartheta = 25^\circ$ , 1<sup>st</sup> set of material constants, grey dots – original data, black line – interpolated line)

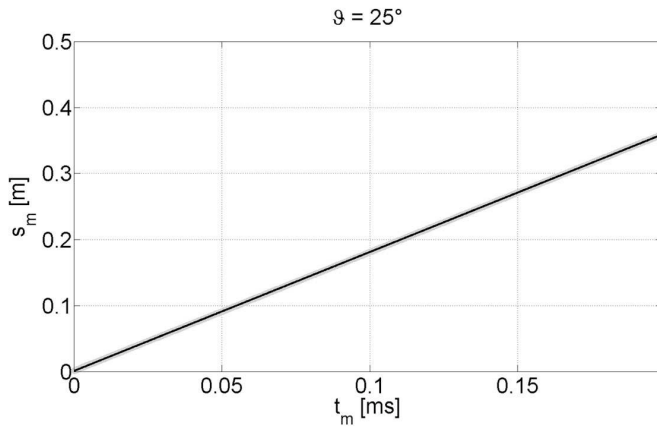


Fig. 7. Distance of R-wave pulse minimum from the loading point vs. time ( $\vartheta = 25^\circ$ , 2<sup>nd</sup> set of material constants, grey dots – original data, black line – interpolated line).

### 5. Comparison of FEA with experimental and theoretical data

Fiber angle dependence of the R-wave velocity is calculated for both sets of the elasticity constants. Numerical results are calculated for interval from  $0^\circ$  to  $180^\circ$  with step  $5^\circ$ . Experimental results were measured for angle  $0^\circ$ ,  $15^\circ$ ,  $30^\circ$ ,  $60^\circ$ ,  $75^\circ$ ,  $90^\circ$ ,  $105^\circ$ ,  $120^\circ$ ,  $150^\circ$ ,  $165^\circ$  and  $180^\circ$ . Theoretical data are calculated for fiber angles  $0^\circ$ ,  $90^\circ$  and  $180^\circ$ . Final results are shown in the fig. 8. The problem is symmetrical with respect to line  $\vartheta = 90^\circ$  where R-wave velocity reaches its minimum.

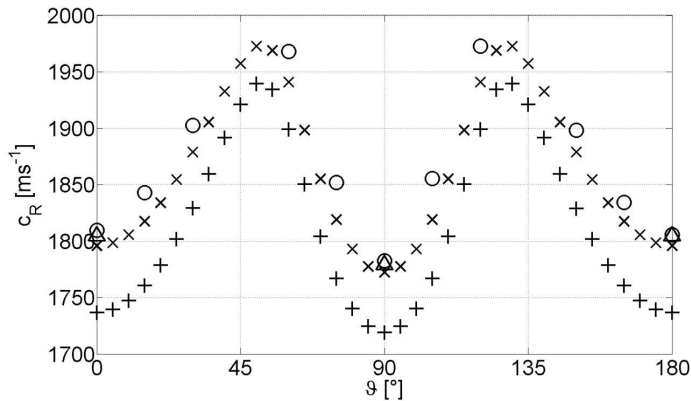


Fig. 8. R-wave velocity vs. fiber angle ( $\times$  – FEM (1<sup>st</sup> set of elasticity constants),  $+$  – FEM (2<sup>nd</sup> set of elasticity constants),  $\circ$  – experiment,  $\triangle$  – analytical)

It is seen from the fig. 8, that FE results for both sets of material constants have the same shape as experimental results. The maximal differences between FEA (first set of constants) and experiment are smaller than 2%. It turns out that the problem solved is very sensitive to shear modulus  $G_{LT}$  (see tab. 1). Accurate setting (positioning) of sensor heads in the experiment is very important as well.

## 6. Conclusion

The paper deals with the investigation of Rayleigh edge wave velocity in a long-fiber reinforced composite panel. The solution is based on numerical (FEA), experimental and analytical approach. It was found that R-wave velocity depends significantly on fiber angles (angle of reinforcement). It was also proven that the problem solved is non-dispersive from the point of view of precision of measurement and the method of calculation. The problem solved is very sensitive to shear modulus  $G_{LT}$  and tolerance on the distance of sensor heads in the experiment.

## Acknowledgements

The work has been supported by the grant project GAAS CR no. A200760611 and GACR no. 101/07/P059.

## References

- [1] S. Abrate, Impact on composite structures, Cambridge university press, 1998.
- [2] J. Červ, Rayleigh (Edge) Waves in a Thin Orthotropic Semi-Infinite Laminate, Proceedings of Eleventh International Congress on Sound and Vibration, 5–8 July 2004, St. Petersburg, Russia, pp. 3 519–3 526.
- [3] J. Červ, R-Waves in Thin Specimens Made of Laminates or Some Anisotropic Metals, Proceedings of the International Scientific Conference, Session 8 – Applied Mechanics, September 7–9, 2005, Ostrava, Czech Republic, pp. 253–256.
- [4] J. Červ, F. Valeš, T. Kroupa, J. Trnka, Wave motion in fibre-reinforced thin orthotropic laminate, Acta Techn. CSAV 52, 2007, Czech Republic, pp. 119–127.
- [5] MSC. Marc Volume A: Theory and User Information, pp. 198–199.
- [6] R. M. Jones, Mechanical of Composite Materials, Scripta Book Company, Washington, D.C., 1975.
- [7] T. Kroupa, J. Červ, V. Laš, Vlny napětí v tenkém pásu s obecnou ortotropií, Proceedings of Computational mechanics 2004, Nečtiny, ZČU Plzeň, Czech Republic, 2004.
- [8] T. Kroupa, J. Červ, F. Valeš, Stress wave propagation in thin long-fiber carbon/epoxy composite panel. Numerical and experimental solutions., Applied and Computational Mechanics 1 (2007) pp. 127–136. ISSN 1802-680X.
- [9] T. Kroupa, R. Zemčík, V. Laš, Identification of composite material properties using non-linear stress-strain relation, Proceedings of Applied mechanics 2006, Srní, Czech Republic, 2006.
- [10] T. Kroupa, R. Zemčík, V. Laš, Progressive failure analysis of orthotropic plate loaded by transverse low-velocity impact, Proceedings of 5<sup>th</sup> International Congress of Croatian Society of Mechanics, Trogir/Split, Croatia, 2006.
- [11] R. Zemčík, J. Červ, V. Laš, Numerical and experimental investigation of stress wave propagation in orthotropic strip, Proceeding of Computational Mechanics 2003, Nečtiny, ZČU Plzeň, 2003.